ELSEVIER

International Journal of Mass Spectrometry 202 (2000) 175–197

International Journal of Mass Spectrometry

Theory of dipolar dc excitation and dc tomography in the rf quadrupole ion trap

Wolfgang R. Plass

Purdue University, Department of Chemistry, West Lafayette, IN 47907-1393, USA

Received 8 December 1999; accepted 28 March 2000

Abstract

A theory of dipolar dc excitation and dc tomography in the rf quadrupole ion trap is presented. The equation of motion for ions subject to a dipolar dc field is written in the form of a Mathieu equation with time independent inhomogeneity and solved analytically. Three cases are considered explicitly: application of continuous dipolar dc fields, application of dipolar pulses for translational excitation of ion motion, and application of dipolar pulses for selective ejection of ions. The effect of monopolar pulses and nonlinear fields is investigated by simulations of ion motion. It is shown that translational excitation of ions by dipolar dc pulses has a near linear response of oscillation amplitude to the voltage of the dipolar dc pulse and is nearly mass independent for a large mass range, provided the pulse width is chosen appropriately. Formulae are given for optimum choice of pulse voltage and width. Dc tomography, a technique which probes ion motion by selective ejection of ions due to the application of short dipolar dc pulses, is shown to be a feasible method for monitoring the secular oscillation of a coherent group of ions, sensitive to even small changes in ion position. (Int J Mass Spectrom 202 (2000) 175–197) © 2000 Elsevier Science B.V.

Keywords: Translational excitation; Ion tomography; Quadrupole ion trap; Mathieu equation; Simulation

1. Introduction

Among the most important capabilities of the rf quadrupole ion trap is the ability to store ions for an extended period of time, to manipulate them and to mass analyze them. Of particular importance is the ease and flexibility in influencing the motion of ions by means of supplementary electric fields, which are superimposed on the rf trapping field. The supplementary fields allow for a variety of destructive [1–6] and nondestructive [7–9] methods of mass analysis, for ion activation and for ion isolation, viz. selective trapping or ejection of ions of particular mass-to-charge ratios or ranges of mass-to-charge ratios [10–12]. Ion isolation can be used to obtain very high sensitivity and is employed in multistage ion isolation and fragmentation experiments (MS^n) [13–15]. Dc fields can be applied as well as ac fields whose frequency matches one of the characteristic frequencies of ions of a particular mass-to-charge ratio, or wave forms which contain a range of frequencies. Depending on amplitude, frequency, and phase of the voltages, depending on the duration of application of

On leave from II. Physikalisches Institut, Justus-Liebig Universität Giessen, 35392 Giessen, Germany. Work done in partial fulfillment of the requirements of the doctoral degree. E-mail: wplass@purdue.edu

PII S1387-3806(00)00241-4

the voltages, and depending on which electrodes they are applied at, ions can be forced to take up or to lose energy, to change their oscillation frequencies or to be ejected from the ion trap.

This article examines the effect of dc voltages applied in dipolar fashion to the two end-cap electrodes of the quadrupole ion trap or in monopolar [16] fashion to either of the end-cap electrodes, while the other is held at ground. The voltage can be applied continuously or as a short pulse.

Dipolar dc pulses have been used in a variety of experiments. Cooks and co-workers have used them for excitation of coherent ion oscillations in nondestructive image current detection experiments [9,17,18]. Lammert et al. have shown that dipolar dc pulses can be used for collisional [19] and surface [20] induced dissociation. They also used them to excite coherent motion of ions and followed their subsequent motion in the trap through position selective laser photoionization [21]. Wang et al. demonstrated that continuous dipolar dc fields can be used for collisional dissociation [22]. Another application of dc pulses is an alternative method of analysis of ion motion in the trap, which can yield a mass spectrum of the trapped ions by determining the oscillation frequencies. Weil et al. showed that, using a technique termed dc tomography, dc pulses can be used to probe the coherent motion of ions in the trap if the pulse voltage is chosen such that ions are either ejected or remain in the trap depending on the state of their motion [23,24]. Zerega and co-workers employed a similar method to determine ion positions in the trap [25,26], however their method requires that the rf trapping voltage be turned off before the ions are ejected by a dc pulse. Then the time of flight to the detector primarily depends on the position and velocity of the ions prior to ejection.

Dipolar dc pulses represent a simple method to eject ions from the trap to detect them or to transfer them to other mass spectrometers. Dawson and Whetten employed mass selective ion storage to generate mass spectra using an ion trap. The detection process for each scan step was realized by pulsing the ions out of the trap into an external detector [1]. Todd and co-workers used the ion trap to conduct ion–molecule reactions and ejected the product ions into a linear quadrupole mass spectrometer for mass analysis [27]. Lubman and co-workers coupled the ion trap to a time-of-flight (TOF) mass spectrometer, but turned off the rf trapping voltage before the starting pulse of the flight time measurement, thus transforming the ion trap into the first stage of the TOF acceleration region [28]. In addition, dual ion trap systems have been examined [26,29]. Here, it is advantageous to use dc pulses both for ejection from the first trap and for ion deceleration after they enter the second trap. Weil et al. have shown from simulations that dc pulses can be employed to increase the trapping efficiency during injection of ions from outside the trap [30]. Note that except in the work of Lubman and co-workers [28] and Zerega and co-workers [25,26] the trapping voltage is not turned off during application of the dc signal.

The analytical treatment of ion motion in the rf trap under influence of the quadrupolar rf field and a dipolar dc field is nontrivial, and to our knowledge no rigorous analytical treatment of this problem has been published, despite the widespread use of dipolar dc fields in the rf ion trap for various purposes. Wuerker et al. [31], Mather and Todd [32], Guan and Marshall [33], and Wang et al. [22] have examined the effect of a dipolar dc in the pseudopotential model only, and Dawson has reported numerical calculations for a few selected conditions [34,35]. In this manuscript, the inhomogeneous Mathieu equation is solved for appropriate initial conditions, and the results are applied to investigate the effects of a continuous dipolar dc and of dipolar dc pulses used for excitation of ions, which are initially at rest, and to investigate a method for probing the coherent motion of an ion cloud. Simulations with the ion trap simulation program ITSIM 5.0 [36,37] extend the results to include nonlinear trapping fields and monopolar dc pulses. Effects of ion–buffer-gas and ion–ion interactions are not included in the treatment.

2. Simulation software

The ion trap simulation program ITSIM 5.0 was used to perform both single-ion trajectory calculations as well as multiple-ion simulations. For single-ion

simulations, the ion was assigned a specific initial position and velocity, or equivalently, a specific oscillation amplitude and phase. Multiple-ion simulations employed 1000 ions, whose initial positions and velocities were determined from distribution functions, appropriate for a cooled ion cloud at the chosen working point in the stability diagram [38,39]. To simulate a coherently oscillating ion cloud, the distribution for position and/or velocity was shifted by a specific value, which determines the amplitude of the coherent oscillation. This assumes that the excitation method does not significantly change the width of the position and velocity distributions, and corresponds to the analytical model which will be derived in this article. The ions' trajectories were calculated using a standard fourth-order Runge–Kutta method. Two different methods for the calculation of the electric field were used: a semi-analytical multipole expansion method and a field interpolation method [40] using an array of potential values on a rectangular mesh precalculated with the Poisson/Superfish software [41]. Although ITSIM allows for the inclusion of both ion–neutral collisions and space-charge effects, neither was used here.

3. Equation of motion

The electric potential in an ion trap with cylindrical symmetry can be expressed in terms of a multipole expansion, which in spherical coordinates (ρ, ϑ, φ) takes the form

$$\Phi(\rho, \vartheta, \varphi, t) = \sum_n \Phi^{(n)}(t) \sum_{l=0}^{\infty} A_l^{(n)} \left(\frac{\rho}{r_N}\right)^l P_l(\cos \vartheta) \tag{1}$$

The sum over n includes all electrodes of the trap, $\Phi^{(n)}(t)$ is the potential on the nth electrode and may be explicitly time dependent, r_N is a normalization radius, $A_l^{(n)}$ are the corresponding dimensionless expansion coefficients, and $P_l(\cos \vartheta)$ is the Legendre polynomial [42] of order l.

The expansion coefficients for the ring electrode can be calculated analytically for the case of an ideal ion trap, the electrode boundaries of which are defined by appropriate hyperbolae [43] and extend into infinity. In that case, only the monopole term and the quadrupole term differ from zero. If the quadrupole ion trap has an inscribed ring electrode radius of r_0 and an end-cap separation of $2z_0$ and the normalization radius is chosen as

$$r_N = r_0 \tag{2}$$

the expansion coefficients are given by

$$A_0^R = \frac{1}{1 + \frac{1}{2}\left(\frac{r_0}{z_0}\right)^2} \tag{3a}$$

$$A_2^R = -\frac{1}{\frac{1}{2} + \left(\frac{z_0}{r_0}\right)^2} \tag{3b}$$

If the trap geometry differs from the ideal geometry, the higher order coefficients are no longer zero. In particular, truncating the electrodes, increasing the end-cap separation without appropriate correction in the hyperbolic shape of the electrodes, or modifying the hyperbolic angle of the trap, as in commercial ion trap mass spectrometers, has been shown to introduce higher even-order terms [4].

The expansion coefficients A_l^{E1} and A_l^{E2} for the end-cap electrodes cannot, in general, be described by a short analytical expression. However, if the end-cap electrodes are identical and arranged symmetrically, symmetry requires that

$$A_l^{E1} = \begin{cases} -A_l^{E2} & l \text{ odd} \\ A_l^{E2} = -\frac{1}{2}A_l^R & l \text{ even} \end{cases} \tag{4}$$

Consequently, if a voltage U^D is applied between the end-caps in a dipolar fashion, i.e. if the potential on the end-caps is given by

$$\Phi^{E1} = -\Phi^{E2} = \tfrac{1}{2}U^D \tag{5}$$

only the odd orders contribute and the terms for both end-caps can be treated by a single term using an expansion coefficient

$$A_l^D = \begin{cases} A_l^{E1} = -A_l^{E2} & l \text{ odd} \\ 0 & l \text{ even} \end{cases} \tag{6}$$

and

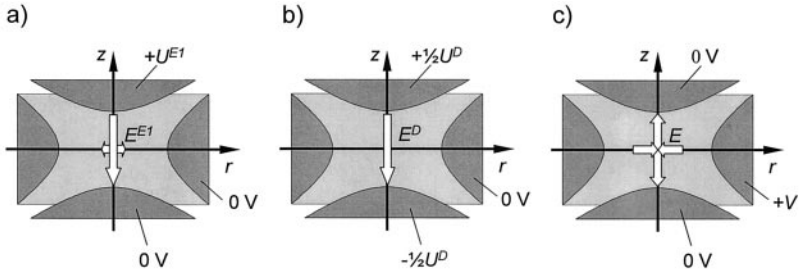

Fig. 1. Schematic view of the quadrupole ion trap and the direction of the electric field for positions on the axis of symmetry and in the central radial plane during application of a positive voltage (a) U^{E1} in monopolar mode, (b) U^D in dipolar mode, and (c) V in quadrupolar mode.

$$\Phi^D = U^D \tag{7}$$

In this work, the dipolar voltage U^D is defined as positive if the dipole is parallel to the z axis, viz. the dipolar electric field is antiparallel to the z axis, and as negative if the dipole is antiparallel to the z axis, viz. the dipolar electric field is parallel to the z axis (Fig. 1).

Values for the expansion coefficients of low order were calculated by a least squares fit of the multipole expansion (1) to the electrostatic potential obtained with the Poisson/Superfish software [41]. The coefficients for hyperbolic traps with ideal geometry and $z_0/r_0 = 1/\sqrt{2}$ as well as for those hyperbolic traps in which the geometry has been changed to $z_0/r_0 = 0.783$ without corresponding change in electrode shape (stretched geometry as used in Finnigan ITD, ITS40 and ITMS ion traps [44]), are shown in Table 1. Calculations for some of these coefficients have also been reported by Gabrielse [45], Beaty [46], Wang and co-workers [4,47], and Splendore et al. [48]. There are minor differences between the reported values, which may be due to different assumptions concerning the truncation of the electrodes. However, these differences are negligible in practice, except in the case of the quadrupole coefficient A_2^R reported by Splendore et al., which differs by some 5% from both the value given here and that given in the work of Wang et al.

Note that although the potential distribution (5) is usually referred to as "dipolar," the resulting fields inside the ion trap contain not only a dipole term, but higher order contributions as well. This is due to the fact that the end-cap electrodes are not flat, parallel surfaces but hyperboloids. However, in the central volume of the ion trap the monopole, dipole and quadrupole terms dominate. The monopole term does not contribute to the electric field and thus does not influence the ion motion. Therefore the ion motion can be described in good approximation using only the dipole and the quadrupole term. Larger deviations can be expected if the ions come close to the electrodes. In this work, the higher order contributions are neglected in the analytical derivation, and computer simulations are used to investigate their effect on ion motion.

In most ion traps a potential consisting of a dc component U and a rf component of amplitude V and frequency $\Omega/(2\pi)$ is applied to the ring electrode. If, in addition, a constant dipolar voltage U^D is applied between the end caps as given by Eq. (5), and all higher order terms are neglected, the potential distri-

Table 1
Table of multipole expansion coefficients for traps of ideal and stretched geometry for a normalization radius $r_N = r_0$

	z_0/r_0	A_2^R	A_4^R	A_6^R	A_1^D	A_3^D	A_5^D
Ideal geometry	$1/\sqrt{2}$	−1	0	0	0.568	0.278	−0.018
Stretched geometry	0.783	−0.895	−0.016	−0.008	0.493	0.239	−0.020

bution inside the trap is given according to Eq. (1) in Cartesian coordinates (x, y, z) by

$$\Phi(x, y, z, t) = [U + V\cos(\Omega t)]\left\{A_0^R + \frac{A_2^R}{r_N^2}\left[z^2 - \frac{1}{2}(x^2 + y^2)\right]\right\} + U^D\frac{A_1^D}{r_N}z \quad (8)$$

Newton's equation of motion for a charged particle of mass m and charge e in an electrostatic field is given by

$$m\frac{d^2\mathbf{r}}{dt^2} = -e\nabla\Phi \quad (9)$$

where $\mathbf{r} = (x, y, z)$ is the position vector of the particle. From Eqs. (8) and (9) one obtains for its components u

$$m\frac{d^2u}{dt^2} = \frac{\gamma eA_2^R}{r_N^2}[U + V\cos(\Omega t)]u + eE^D \quad (10)$$

where

$$\gamma = \begin{cases} +1 & u = x \text{ or } u = y \\ -2 & u = z \end{cases} \quad (11)$$

and the dipolar electric field is given by

$$E^D = -\frac{A_1^D U^D}{r_N} \quad (12)$$

With the substitutions

$$\xi = \frac{\Omega t}{2} \quad (13a)$$

$$a_u = -\frac{4\gamma eA_2^R U}{mr_N^2\Omega^2} \quad (13b)$$

$$q_u = \frac{2\gamma eA_2^R V}{mr_N^2\Omega^2} \quad (13c)$$

$$f = \frac{4eE^D}{m\Omega^2} \quad (13d)$$

the equation of motion (10) can be cast into the form of the inhomogeneous Mathieu equation

$$\frac{d^2u}{d\xi^2} + [a_u - 2q_u\cos(2\xi)]u = f \quad (14)$$

Stable solutions are given by [49,50]

$$u(\xi) = \lambda ce_{\beta_u}(\xi) + \mu se_{\beta_u}(\xi) + u^P(\xi) \quad (15)$$

where $ce_{\beta_u}(\xi)$ and $se_{\beta_u}(\xi)$ are the even and odd Mathieu functions of fractional order β_u

$$ce_{\beta_u}(\xi) = \sum_{n=-\infty}^{+\infty} C_{2n,u}\cos[(2n + \beta_u)\xi] \quad (16a)$$

$$se_{\beta_u}(\xi) = \sum_{n=-\infty}^{+\infty} C_{2n,u}\sin[(2n + \beta_u)\xi] \quad (16b)$$

and $u^P(\xi)$ is a particular solution of the inhomogeneous Mathieu equation and λ and μ are arbitrary constants, which determine amplitude and phase of the motion. The coefficients $C_{2n,u}$ describe the relative strength of each term. Both β_u and $C_{2n,u}$ are determined by a_u and q_u and can be calculated using a continued fraction expression [49,51]. A particular solution can be found from [50]

$$u^P(\xi) = \int^{\xi}\frac{f}{W_0}[ce_{\beta_u}(\tau)se_{\beta_u}(\xi) - se_{\beta_u}(\tau)ce_{\beta_u}(\xi)]\,d\tau \quad (17)$$

where W_0 is the time-independent [51] Wronskian of $ce_{\beta_u}(\xi)$ and $se_{\beta_u}(\xi)$

$$W_0 = \sum_{n=-\infty}^{+\infty} C_{2n,u}\sum_{n=-\infty}^{+\infty} C_{2n,u}(2n + \beta_u) \quad (18)$$

In the case where ions are subject to the dipolar dc field only during the time interval $t = t_0$ to $t = t_0 + \Delta t$, corresponding to $\xi = \xi_0$ to $\xi = \xi_0 + \Delta\xi$, three subsequent time intervals have to be considered, each of which may have a different equation of motion

$$\frac{d^2u_1}{d\xi^2} + [a_u - 2q_u\cos(2\xi)]u_1 = 0 \qquad \xi < \xi_0 \quad (19)$$

$$\frac{d^2u_2}{d\xi^2} + [a_u - 2q_u\cos(2\xi)]u_2 = f \qquad \xi_0 \le \xi \le \xi_0 + \Delta\xi \quad (20)$$

$$\frac{d^2u_3}{d\xi^2} + [a_u - 2q_u \cos(2\xi)]u_3 = 0 \qquad \xi > \xi_0 + \Delta\xi \tag{21}$$

Continuity of ion position and velocity requires

$$u_1(\xi_0) = u_2(\xi_0) \tag{22a}$$

$$\dot{u}_1(\xi_0) = \dot{u}_2(\xi_0) \tag{22b}$$

and

$$u_2(\xi_0 + \Delta\xi) = u_3(\xi_0 + \Delta\xi) \tag{23a}$$

$$\dot{u}_2(\xi_0 + \Delta\xi) = \dot{u}_3(\xi_0 + \Delta\xi) \tag{23b}$$

where

$$\dot{u}(\xi_0) = \left.\frac{du(\xi)}{d\xi}\right|_{\xi=\xi_0}$$

The solution of Eq. (19) is

$$u_1(\xi) = \lambda_i ce_{\beta_u}(\xi) + \mu_i se_{\beta_u}(\xi) \tag{24}$$

The constants λ_i and μ_i can be chosen freely to accommodate any initial condition. Note that for reasons of simplicity Eqs. (8) and (19)–(21) do not allow for an arbitrary phase of the rf at time $t = 0$. Nevertheless the treatment is valid in general, since the point of time of application of the dipolar dc can be chosen arbitrarily, viz. at an arbitrary rf phase.

The solution of Eq. (20) together with the conditions (22) gives

$$u_2(\xi) = \lambda_2(\xi) ce_{\beta_u}(\xi) + \mu_2(\xi) se_{\beta_u}(\xi) \tag{25}$$

where

$$\lambda_2(\xi) = \lambda_i + \frac{f}{W_0} \sum_{n=-\infty}^{+\infty} \frac{C_{2n,u}}{2n + \beta_u} \{\cos[(2n + \beta_u)\xi] - \cos[(2n + \beta_u)\xi_0]\} \tag{26a}$$

$$\mu_2(\xi) = \mu_i + \frac{f}{W_0} \sum_{n=-\infty}^{+\infty} \frac{C_{2n,u}}{2n + \beta_u} \{\sin[(2n + \beta_u)\xi] - \sin[(2n + \beta_u)\xi_0]\} \tag{26b}$$

The solution of Eq. (21) together with (23) is

$$u_3(\xi) = \lambda_f ce_{\beta_u}(\xi) + \mu_f se_{\beta_u}(\xi) \tag{27}$$

where

$$\lambda_f = \lambda_2(\xi_0 + \Delta\xi) \tag{28a}$$

$$\mu_f = \mu_2(\xi_0 + \Delta\xi) \tag{28b}$$

For the discussion in the following sections it is convenient to re-substitute the time variable and to define the angular frequencies of ion motion

$$\omega_{n,u} = (n + \tfrac{1}{2}\beta_u)\Omega \tag{29}$$

$$\Omega_W = \frac{1}{2}\,\Omega W_0 = \sum_{n=-\infty}^{+\infty} C_{2n,u} \sum_{n=-\infty}^{+\infty} C_{2n,u}\omega_{n,u} \tag{30}$$

There are different measures for the efficiency of the applied dc, and which of them is appropriate depends on the purpose for which the dc signal is used. If it is used to eject all ions or a part of the ion population from the trap, the maximum excursion of the ions after excitation is the value of interest. The same is true for the case when the dc pulse is used to remove energy from the ions, e.g. after ion injection in order to provide oscillations that do not exceed the volume of the ion trap. For image current detection experiments [9] however, usually only the secular oscillation is of interest and the micromotion can be neglected, because the micromotion frequencies are filtered out by the detection electronics. Then only the amplitude of the secular oscillation after excitation needs to be considered. Nevertheless the effect of the micromotion during the excitation process itself should not be neglected.

In order to obtain the amplitude of the ion oscillation in the absence of a dipolar dc field, Eq. (24) or (27) is rewritten in the form

$$u(t) = \sqrt{\lambda^2 + \mu^2} \sum_{n=-\infty}^{+\infty} C_{2n,u} \cos(\omega_{n,u}t + \varphi) \tag{31}$$

where φ is the phase of ion motion and can be calculated from

$$\varphi = -\arctan\left(\frac{\mu}{\lambda}\right) \tag{32}$$

The amplitude $\hat{u}$ of the oscillation, viz. the maximum excursion of the ion from the center of the ion trap, is thus given by

$$\hat{u} = \max_t|u(t)| = \sqrt{\lambda^2 + \mu^2} \sum_{n=-\infty}^{+\infty} |C_{2n,u}| \tag{33}$$

It should be noted here that $u(t)$ does not in general take the value $\hat{u}$. If β_u is rational, $\beta_u = r/s$ with r and s integers, $u(t)$ is periodic [49], but at the extremum of the secular oscillation the micomotion terms may not add up with the same sign. If β_u is irrational, $u(t)$ is not periodic. For most practical purposes, however, $u(t)$ comes sufficiently close to its extremum after a few secular oscillations [7]. The secular oscillation is given by the term of zero order in Eq. (31)

$$u^{\text{sec}}(t) = \sqrt{\lambda^2 + \mu^2}\, C_{0,u} \cos(\omega_{0,u}t + \varphi) \tag{34}$$

Consequently, its amplitude is

$$\hat{u}^{\text{sec}} = \sqrt{\lambda^2 + \mu^2}\, |C_{0,u}| \tag{35}$$

For practical purposes, it is often convenient not to calculate the coefficients and frequencies of ion motion in Eq. (31) to high precision, but rather to use approximations. In the pseudopotential model [31,51,52], which assumes $a_u \ll q_u \ll 1$, the motion is approximated by the sum of the secular oscillation, which can be interpreted as the motion of the ion in a time-averaged harmonic potential, and a single term which represents the micromotion. In this approximation, the ion position is given by

$$\bar{u}(t) = [\lambda \cos(\bar{\omega}_u t) + \mu \sin(\bar{\omega}_u t)] \cdot [1 - \tfrac{1}{2} q_u \cos(\Omega t)] \tag{36}$$

The amplitude in the pseudopotential model is thus

$$\hat{\bar{u}} = \sqrt{\lambda^2 + \mu^2}\, (1 + \tfrac{1}{2} q_u) \tag{37}$$

Note that commonly only the secular oscillation is considered in the pseudopotential model. Only a few authors [53,54] have included the correction for the micromotion, and the corresponding model has been termed the modified pseudopotential model [53]. Neglecting the micromotion completely leads to less accurate results, particularly in problems which depend on the velocity rather than just the position of the ion [53]. Only the modified pseudopotential model will be used in this work. In Eq. (37) the factor $(1 + \frac{1}{2} q_u)$ results from inclusion of the micromotion. The secular frequency is approximated by

$$\bar{\omega}_u = \tfrac{1}{2} \sqrt{a_u + \tfrac{1}{2} q_u^2}\, \Omega \tag{38}$$

Wuerker et al. have verified this approximation experimentally and determined it to be accurate within 1% for $q_z \leq 0.4$, $a_z = 0$ [31]. One finds

$$\begin{aligned} \Omega_W &\approx (C_{-2,u} + C_{0,u} + C_{2,u}) \\ &\quad \cdot (C_{-2,u}\omega_{-2,u} + C_{0,u}\omega_{0,u} + C_{2,u}\omega_{2,u}) \\ &\approx \bar{\omega}_u(1 - \tfrac{1}{4} q_u^2) \end{aligned} \tag{39}$$

4. Continuous dipolar dc

Equation (25) describes the motion of an ion subject to a continuous dipolar dc signal. Re-substitution and application of trigonometric addition theorems yields

$$u_2(t) = \lambda_i \sum_{n=-\infty}^{+\infty} C_{2n,u} \cos(\omega_{n,u}t) + \mu_i \sum_{n=-\infty}^{+\infty} C_{2n,u} \sin(\omega_{n,u}t) + \frac{eE^D}{m\Omega_W} \sum_{n=-\infty}^{+\infty} \sum_{m=-\infty}^{+\infty} \frac{C_{2n,u}C_{2m,u}}{\omega_{n,u}} \{\cos[(n-m)\Omega t] - \cos[\omega_{m,u}(t - t_0) - (n-m)\Omega t_0]\} \tag{40}$$

Thus the ion oscillation is the sum of the oscillation without application of the dipolar dc and an additional term. The meaning of the different summands can be illustrated by applying the pseudopotential approximation to equation (40)

$$\bar{u}_2(t) = \left(\lambda_i \cos(\bar{\omega}_u t) + \mu_i \sin(\bar{\omega}_u t) + \frac{eE^D}{(1 - \frac{1}{4} q_u^2) m \bar{\omega}_u^2} \cdot \{1 - \cos[\bar{\omega}_u(t - t_0)]\} \right) [1 - \tfrac{1}{2} q_u \cos(\Omega t)] \tag{41}$$

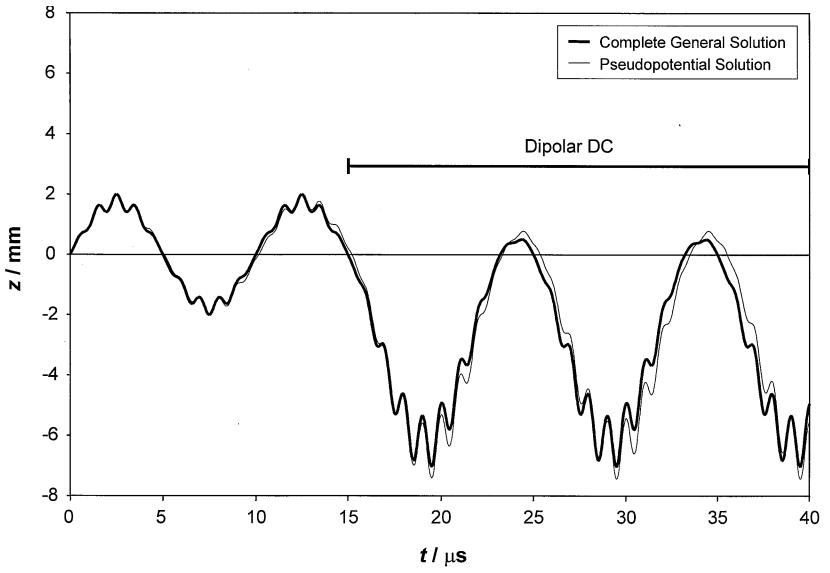

Fig. 2. Example of the effect of a continuous dipolar dc on the motion of an ion with mass-to-charge ratio 100 Th at $q_z = 0.278$, $a_z = 0$ ($\beta_z = 0.2$) in an ideal trap with $r_0 = 10$ mm, $z_0 = 7.07$ mm, and $\Omega/(2\pi) = 1$ MHz. The amplitude of the ion oscillation before application of the dipolar dc is 2 mm, the dc voltage is +20 V. Both the complete general solution (40) and the pseudopotential approximation (41) are shown.

The third term in the sum is due to the perturbation of the dipolar dc. It approximately has the effect of shifting the center of oscillation by a distance given by the time-independent factor of the third term. Differing from the case of a dipolar rf contribution [48], the shifted oscillation is not symmetric. Since the rf field but not the dipolar dc field vanishes in the center of the trap, the micromotion at the turning point closer to the center of the trap is weaker than the micromotion at the opposite turning point. This effect is illustrated in Fig. 2, which shows the motion of an ion with a mass-to-charge ratio of 100 Th (the unit Thomson is defined as [55] 1 Th = 1 u/e_0, where u is the atomic mass unit and e_0 the elementary charge) held at $q_z = 0.278$, $a_z = 0$ under the influence of a supplementary dipolar dc of +20 V. The plots show the results of Eq. (40) and its approximation (41). The small deviations between the results are mainly due to the slightly different secular frequencies, which were calculated from Eqs. (29) and (38), respectively. Obviously, application of the dipolar dc can significantly increase the kinetic energy of the ion. This observation led Wang et al. to the excitation method termed "nonresonance excitation," in which ions are excited for collision induced dissociation (CID) by a dipolar dc field [22]. Since collisions with buffer gas atoms result in subsequent cooling of the ion population, the direction of the dipolar field is reversed with a frequency which roughly corresponds to the cooling time. Thus the ion is excited repetitively.

Wang et al. also showed that the dependence of the spatial shift on the mass-to-charge ratio can be used to remove ions above a certain mass from the ion trap. If the ion initially is at rest in the center of the trap ($\lambda_i = \mu_i = 0$), according to Eq. (41) the maximum excursion from the trap center will be

$$\bar{u}_2^{\max} = \frac{2|eE^D|}{(1 - \frac{1}{2}q_u)m\bar{\omega}_u^2} \tag{42}$$

Neglecting the correction factor due to micromotion and assuming $a_u = 0$, the expression can be simplified to

$$\bar{u}_2^{\max} = \frac{2|eE^D|}{m\bar{\omega}_u^2} = 4\,\frac{m}{|e|}\left(\frac{r_N^2\Omega}{\gamma A_2^R V}\right)^2 |E^D| \tag{43}$$

The magnitude of the excursions is therefore approximately proportional to the mass-to-charge ratio of the ion. Thus all ions with a mass-to-charge ratio larger than a certain value determined by the rf amplitude, the dc voltage and the trap geometry will either be

ejected from the trap or impinge on the trap electrodes. Therefore, in addition to the low-mass-cutoff due to the properties of the dynamic trapping a "high-mass-cutoff" due to the static dipolar field can be established and a particular mass range selected. The shift in the center of oscillation during application of a dipolar dc has also been used by Nappi et al. for single-ended image current detection [56]. It was found that the image current signal on the detector electrode increased if the oscillation center was shifted toward the detector electrode.

5. Dipolar dc pulse

In the following sections, the effect of the application of a dc pulse of length Δt on the ion motion after the pulse is investigated. Note that an ideal rectangular pulse is assumed, while in real experiments a pulse will always have a finite rise and fall time and ripple. However these deviations from the ideal pulse form can be made small compared to the total pulse amplitude and width, and in that case no significantly different results will be obtained.

Re-substitution transforms Eq. (27) into

$$u_3(t) = \lambda_f \sum_{n=-\infty}^{+\infty} C_{2n,u} \cos(\omega_{n,u} t) + \mu_f \sum_{n=-\infty}^{+\infty} C_{2n,u} \sin(\omega_{n,u} t) \quad (44)$$

where

$$\lambda_f = \lambda_i + \frac{eE^D}{m\Omega_W} \sum_{n=-\infty}^{+\infty} \frac{C_{2n,u}}{\omega_{n,u}} \{\cos[\omega_n(t_0 + \Delta t)] - \cos(\omega_{n,u} t_0)\} \quad (45a)$$

$$\mu_f = \mu_i + \frac{eE^D}{m\Omega_W} \sum_{n=-\infty}^{+\infty} \frac{C_{2n,u}}{\omega_{n,u}} \{\sin[\omega_n(t_0 + \Delta t)] - \sin(\omega_{n,u} t_0)\} \quad (45b)$$

Clearly, the ion can take up energy or lose energy to the electric field, thus increasing or decreasing its oscillation amplitude, depending on its oscillation amplitude and phase at the time at which the pulse is applied and on the dipolar dc voltage. An example for both cases is shown in Fig. 3. A dipolar pulse with an amplitude of +6.12 V and width of 5 μs is applied during the oscillation of an ion with a mass-to-charge ratio of 100 Th held at $q_z = 0.278$, $a_z = 0$ in an ideal trap with $\Omega/(2\pi) = 1$ MHz. Depending on whether the pulse is applied during the downwards motion (i.e. motion parallel to the dc field) or upwards motion (i.e. motion antiparallel to the dc field) of the ion, the oscillation amplitude is increased or decreased. The pulse amplitude of +6.12 V was calculated according to Eqs. (45) such that in the latter case all kinetic energy is removed from the ion.

To gain a more detailed understanding of the dependence of the resulting oscillation amplitude on the amplitude and phase of the initial ion motion, the phase of the rf, and the pulse amplitude, the oscillation amplitude can be calculated from Eqs. (33) and (45)

$$\hat{u}_3 = \sum_{n=-\infty}^{+\infty} |C_{2n,u}| \left\{ \lambda_i^2 + \mu_i^2 + 4\left(\frac{eE^D}{m\Omega_W}\right) \sum_{n=-\infty}^{+\infty} \frac{C_{2n,u}}{\omega_{n,u}} \{-\lambda_i \sin[\omega_{n,u}(t_0 + \tfrac{1}{2}\Delta t)] + \mu_i \cos[\omega_{n,u}(t_0 + \tfrac{1}{2}\Delta t)]\} \sin(\tfrac{1}{2}\omega_{n,u}\Delta t) + 4\left(\frac{eE^D}{m\Omega_W}\right)^2 \sum_{n=-\infty}^{+\infty} \sum_{m=-\infty}^{+\infty} \frac{C_{2n,u}C_{2m,u}}{\omega_{n,u}\omega_{m,u}} \cos[(n-m)\Omega (t_0 + \tfrac{1}{2}\Delta t)] \sin(\tfrac{1}{2}\omega_{m,u}\Delta t) \sin(\tfrac{1}{2}\omega_{m,u}\Delta t) \right\}^{1/2} \quad (46)$$

The amplitude after the pulse is determined by four terms. The first two terms represent the energy contained in the motion prior to the application of the pulse. The last two terms are due to energy exchange with the electric field. Their meaning becomes clear in the pseudopotential model, where Eq. (46) reduces to

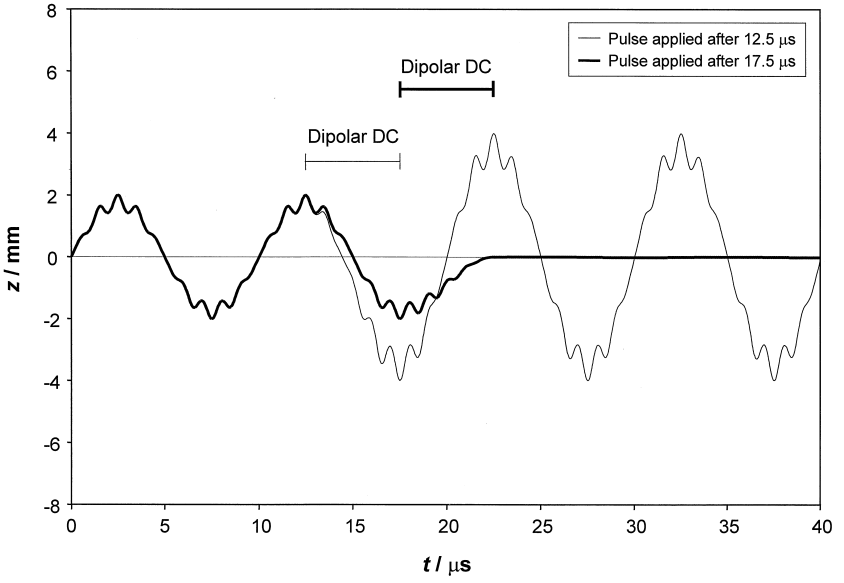

Fig. 3. Motion of an ion with a mass-to-charge ratio of 100 Th at $q_z = 0.278$, $a_z = 0$ ($\beta_z = 0.2$) in an ideal trap with $r_0 = 10$ mm, $z_0 = 7.07$ mm, and $\Omega/(2\pi) = 1$ MHz under the influence of a dipolar dc pulse applied during the downward motion (motion parallel to the dc field; start at 12.5 μs) or upward motion (motion antiparallel to the dc field; start at 17.5 μs). The amplitude of the ion oscillation before application of the dipolar dc is 2 mm, the dc width is 5 μs and the pulse voltage is +6.12 V.

$$\hat{\bar{u}}_3 = (1 + \tfrac{1}{2}q_u)\left\{\lambda_i^2 + \mu_i^2 + 4\left(\frac{eE^D}{(1 - \tfrac{1}{4}q_u^2)m\bar{\omega}_u^2}\sin(\tfrac{1}{2}\bar{\omega}_u\Delta t)\right)\frac{\dot{\bar{u}}_1^{\mathrm{sec}}(t_0 + \tfrac{1}{2}\Delta t)}{\bar{\omega}_u} + 4\left(\frac{eE^D}{(1 - \tfrac{1}{4}q_u^2)m\bar{\omega}_u^2}\sin(\tfrac{1}{2}\bar{\omega}_u\Delta t)\right)^2\right\}^{1/2} \quad (47)$$

where

$$\dot{\bar{u}}_1^{\mathrm{sec}}(t_0 + \tfrac{1}{2}\Delta t) = -\lambda_i\bar{\omega}_u\sin[\bar{\omega}_u(t_0 + \tfrac{1}{2}\Delta t)] + \mu_i\bar{\omega}_u\cos[\bar{\omega}_u(t_0 + \tfrac{1}{2}\Delta t)] \quad (48)$$

is the secular ion velocity at $t = t_0 + \frac{1}{2}\Delta t$. The fourth term is independent of the amplitude or phase of ion motion, while the third term describes the ion motion dependent energy exchange with the electric field. If the ion is moving in the direction of the dipolar field, i.e. if velocity and field are parallel, this term is positive; if the ion is moving against the field, this term is negative. However, the third term in Eq. (46) is, to a good approximation, proportional to the secular velocity only, i.e. the term of order zero, not to the total velocity which also contains the contribution of the micromotion. The reason for this is that the contribution of summands of higher order is much weaker in the third term of Eq. (46) than in the ion velocity, where the frequencies appear in the numerator and not in the denominator. Therefore, the amplitude after the pulse is, to a good approximation, a measure for the amplitude and phase of the secular oscillation, if the fourth term can be made sufficiently small. This unique property of the dc pulse excitation will be dealt with later.

6. Dipolar dc pulse excitation

An ion initially at rest ($\lambda_i = \mu_i = 0$) can be forced into oscillation, the amplitude of which is

determined by the voltage of the dc pulse, its width and its phase relative to the rf. During normal operation of the ion trap, ions created in the trap or injected from outside are cooled to the central region of the ion trap by collisions with light buffer gas atoms. Due to the thermal energy of the buffer gas atoms and space charge effects, the ion cloud has a finite width which, in commercial ion trap mass spectrometers, is of the order of 1 mm [57,58]. While for these ions $\lambda_i \neq 0$ and/or $\mu_i \neq 0$, the ion cloud can nevertheless be excited into coherent oscillations, and the average ion will behave similarly to an ion which resides at the center of the trap prior to the dc pulse, provided the increase in kinetic energy due to the pulse is large compared to the ion's initial kinetic energy.

For working points corresponding to small values of β_u, the contributions of higher orders in Eq. (46) are negligible and the rf phase dependence vanishes. In the pseudopotential well model one has

$$\hat{\bar{u}}_3 = \frac{2}{1 - \frac{1}{2} q_u} \frac{|eE^D \sin(\frac{1}{2} \bar{\omega}_{0,u} \Delta t)|}{m \bar{\omega}_{0,u}^2} \tag{49}$$

Thus, the dc pulse is without effect for a pulse width which is an integral multiple of the inverse secular frequency, i.e.

$$\Delta t = \nu \frac{2\pi}{\omega_{0,u}} = \nu \frac{2}{\beta_u} \left(\frac{2\pi}{\Omega} \right) \qquad \nu = 1, 2, 3, \ldots \tag{50}$$

To avoid mass discrimination effects because of the frequency dependence, the pulse width should be small compared to the period of one secular oscillation. In practice, this condition can be fulfilled for a reasonable mass range if the pulse width does not exceed two rf periods. For short dc pulses $\Delta t \ll 2\pi/\omega_{0,u}$, $a_u = 0$, and neglecting the correction factor for micromotion, Eq. (49) can be further simplified to yield

$$\hat{\bar{u}}_3 \approx \frac{|eE^D|}{m \bar{\omega}_u} \Delta t = \sqrt{2} \frac{r_N^2}{|\gamma A_2^R| V} |E^D| \Omega \Delta t \tag{51}$$

The resulting amplitude is proportional to the dipolar electric field and roughly proportional to the pulse width. For a given ion mass, the amplitude is inversely proportional to the secular frequency, but because, for a given rf voltage, the secular frequency is roughly inversely proportional to the ion mass, the amplitude of ion motion is nearly independent of ion mass at fixed rf trapping voltage.

At higher β_u, higher orders can no longer be ignored. Then the oscillation amplitude becomes dependent on the phase of the rf driving frequency. Dawson and Lambert [35] and later Todd and Waldren [59–62] observed this problem in experimental studies and showed that it may lead to mass discrimination effects. There are several ways to deal with the dependence on the rf phase. To obtain reproducible results, the dc pulse can be phase locked with the rf. However, since according to Eq. (46) the effect of the rf phase will, in general, depend on the ion frequency, this method should not be used for experiments involving ions of different mass. For these experiments, the results could be averaged over a number of different rf-phases. More conveniently, the optimum choice of the pulse width can also reduce the effect of the rf phase dependence. In the following section the influence of the pulse width on the rf phase dependence will be investigated, starting with considerations for ions of one mass.

Fig. 4 shows the dependence of the oscillation amplitude after the pulse on the pulse width Δt for $q_u = 0.3$, $a_u = 0$. The amplitude is given in units relative to the linear case (51). Because of the dependence on the rf phase, a range of amplitudes is obtained when the start time t_0 is varied over one rf cycle. Fig. 4 gives the maximum and the minimum amplitude as calculated from Eq. (46). Also shown is the result of the pseudopotential approximation (49). The dependence on the rf phase decreases with increasing pulse width and vanishes for a value which is slightly larger than the rf period. It increases again for larger pulse widths, and vanishes for a second time for a value slightly larger than two rf periods. The overall importance of the rf phase decreases for large pulse widths. However, for large pulse widths, the amplitude decreases, and the contribution of the secular term in Eq. (46) vanishes when condition (50) is reached. A similar behavior can be observed for larger q values. Fig. 5 shows the dependence of the

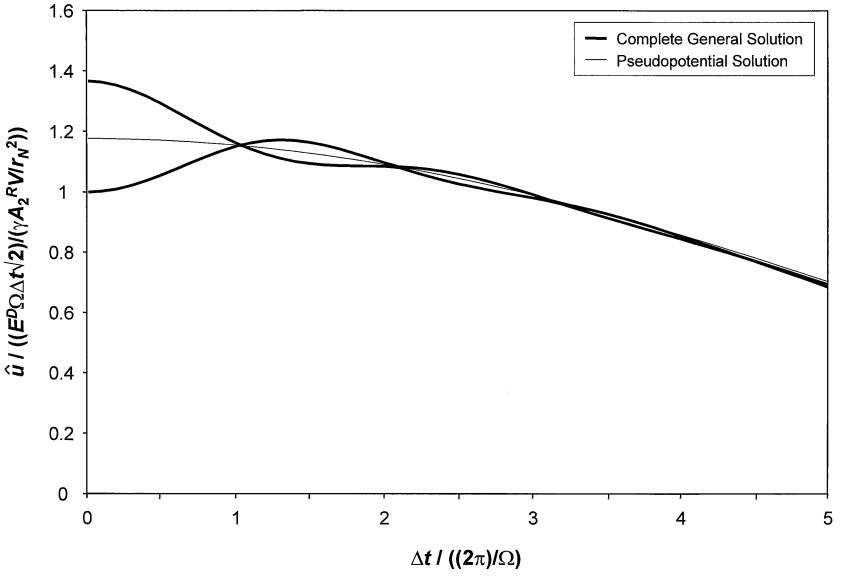

Fig. 4. Dependence of the oscillation amplitude after a dipolar dc pulse on the pulse width Δt for $q_u = 0.3$, $a_u = 0$. The amplitude is given in units relative to Eq. (51). Both the maximum and the minimum amplitude during one rf cycle as calculated from Eq. (46) and the pseudopotential approximation calculated from Eq. (49) are shown.

oscillation amplitude on the pulse width Δt for $q_u = 0.85$, $a_u = 0$. Here, the rf phase dependence of the oscillation amplitude vanishes for a pulse width of about 1.7 rf periods. But condition (50) is reached already for a pulse width of about 2.5 rf periods because of the larger secular frequency at this work-

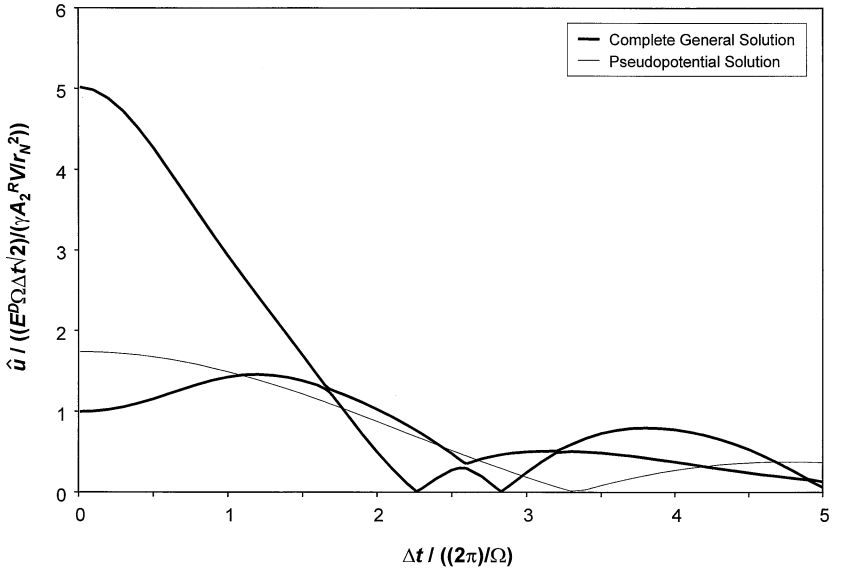

Fig. 5. Dependence of the oscillation amplitude after a dipolar dc pulse on the pulse width Δt for $q_u = 0.85$, $a_u = 0$. The amplitude is given in units relative to Eq. (51). Both the maximum and the minimum amplitude during one rf cycle as calculated from Eq. (46) and the pseudopotential approximation calculated from Eq. (49) are shown.

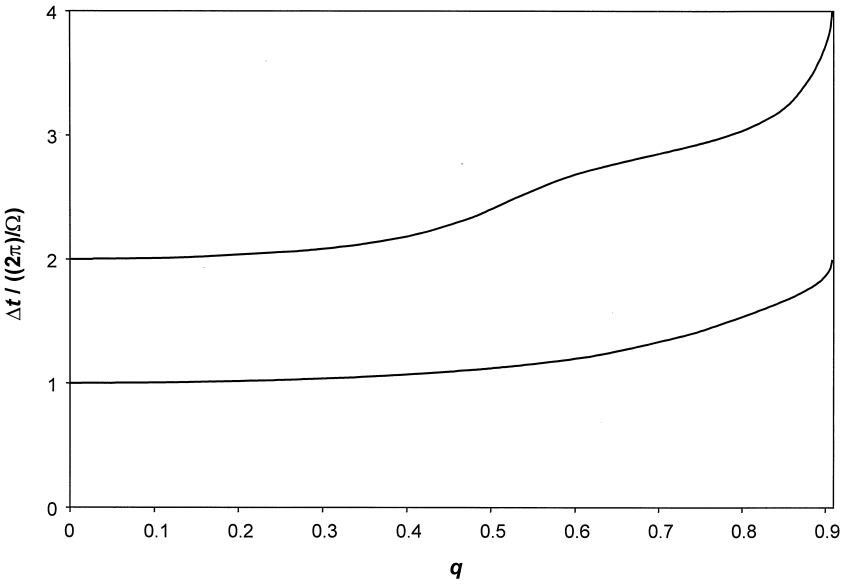

Fig. 6. Optimum pulse widths in units of the rf period as a function of q_u for $a_u = 0$ as calculated from Eq. (52).

ing point. This indicates that an optimum pulse width can be found for values between 1 and 2 rf periods.

Analysis of Eq. (46) shows that it is the mutual compensation of higher order terms, which leads to a vanishing of the rf phase dependence. In particular, the two terms which contain the product $C_{0,u}C_{2,u}$ or $C_{0,u}C_{-2,u}$ are of importance. They compensate each other under the condition

$$\frac{C_{0,u}}{\omega_{0,u}} \sin\left(\frac{1}{2}\,\omega_{0,u}\Delta t\right)\left[\frac{C_{-2,u}}{\omega_{-1,u}} \sin\left(\frac{1}{2}\,\omega_{-1,u}\Delta t\right) + \frac{C_{2,u}}{\omega_{1,u}} \sin\left(\frac{1}{2}\,\omega_{1,u}\Delta t\right)\right] = 0 \qquad (52)$$

The result of a numerical calculation for these pulse widths as a function of q_u for $a_u = 0$ is given in Fig. 6. For small q_u, the optimum values are integral multiples of the rf period. For larger q_u, the optimum values increase because of the asymmetry in the coefficients $C_{2n,u}$. However, the dependence on q_u is weak, and significantly different values are required only for working points close to the stability boundary at $q_u = 0.908$. A pulse width of 1–1.1 times the rf period should therefore sufficiently minimize the dependence of oscillation amplitude on the rf phase for most practical purposes.

Fig. 7 shows the maximum and the minimum amplitude as a function of q_u for $a_u = 0$ and $\Delta t = 1.1(2\pi/\Omega)$. The amplitude increases slightly, but almost linearly with q_u, and a significant rf dependence is observed only for $q_u > 0.6$. The maximum and the minimum amplitudes of the secular oscillation are also shown. It is almost independent of q_u, viz. the ion mass, and the rf phase for $q_u < 0.6$. Thus, excitation of ions by dipolar dc pulses for a variety of experiments is feasible, in particular for those where broadband characteristics are required, viz. those in which the ions must be excited to the same oscillation amplitude independently of their mass.

This property is hardly changed if more realistic fields instead of the pure quadrupolar trapping field with a dipolar dc superposition are considered. Fig. 8 shows the oscillation amplitude after the dc pulse as a function of pulse voltage for dipolar pulses in a trap without high order fields and for dipolar and monopolar pulses in a trap with high order fields. Simulations were obtained using the ion trap simulation program ITSIM for an ion with a mass-to-charge ratio of 100

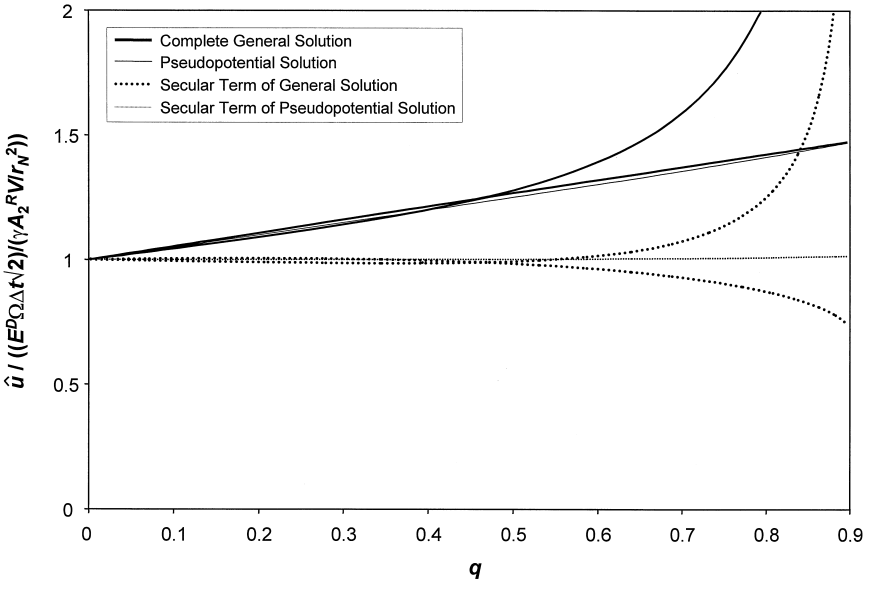

Fig. 7. Maximum and minimum oscillation amplitudes as a function of q_u for $a_u = 0$ calculated for a pulse width of $\Delta t = 1.1(2\pi/\Omega)$. The amplitude is given in units relative to Eq. (51). The total amplitudes including micromotion as well as the amplitudes of the secular oscillation only are shown. The results of the pseudopotential solution are also given.

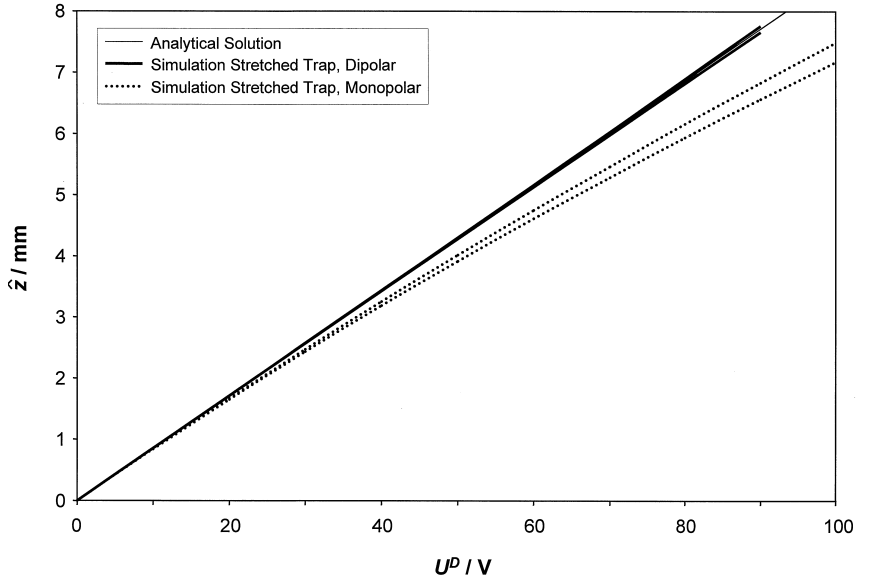

Fig. 8. Dependence of oscillation amplitude as a function of pulse voltage for an ion with a mass-to-charge ratio of 100 Th at $q_z = 0.3$, $a_z = 0$ in a stretched trap with $r_0 = 10$ mm, $z_0 = 7.83$ mm, and $\Omega/(2\pi) = 1$ MHz. The maximum and the minimum amplitude for dipolar and positive monopolar pulses with a width of 1.04 μs as obtained by simulations are shown and compared with the results of Eq. (46), which includes only a quadrupolar rf field and a dipolar dc field.

Th at $q_z = 0.3$, $a_z = 0$, which oscillates along the z axis under the influence of a 1.04 μs dipolar dc pulse with variable amplitude in a stretched ion trap with $r_0 = 10$ mm and $z_0 = 7.83$ mm. Both the multipole expansion method using the coefficients given in Table 1 and the field interpolation method were used, but differences in the results of the two methods were negligible. The results are shown in Fig. 8 and compared with the analytical solution as calculated from Eq. (46). Due to the optimized pulse width, the oscillation amplitude after the pulse is nearly phase independent and increases linearly with pulse voltage. The influence of the higher order field contributions is small. This finding is consistent with the work of Gaboriaud et al. [63], who calculated an efficiency factor for the strength of a dipolar voltage during resonance excitation, which takes into account the higher odd-order terms of the electric potential. They showed that the efficiency factor varies only slightly with average ion energy, viz. distance from the trap center. The reason for the weak dependence on the higher odd-order fields of the dipolar pulse, here in particular the hexapole, is that these only contribute significantly at larger distances from the trap center. If the pulse width is smaller than a quarter of the secular oscillation period, the dipolar pulse is turned off before the ion reaches regions with significant higher order fields. The higher even-order terms of the rf field due to the stretched geometry hardly affect the ion motion, because, as has been shown earlier, dc pulse excitation is a broadband method and hence not influenced by small changes in ion frequencies. This is an important advantage over single-frequency resonance excitation, where higher order fields shift the ion frequency out of resonance with the excitation frequency for increasing oscillation amplitude, therefore the excitation frequency has to be tuned for a given excitation voltage.

Also shown in Fig. 8 are the results of simulations for monopolar excitation in a stretched trap, where a positive pulse was applied to one end-cap electrode only, leaving the other grounded. The polarity of the pulse cor-responds to the “pulse-out” mode in the experiments of Todd and Waldren [59]. Here, the dependence of oscillation amplitude on pulse voltage is nonlinear, and the dependence on rf phase is much stronger. This result can be explained by the quadrupole contribution in the multipole expansion for the monopolar pulse according to Eq. (4). During the pulse the ion movement is modified by the additional quadrupolar dc voltage, which significantly changes the ion’s frequency. The larger the pulse voltage is, the larger the quadrupolar dc, and the larger the deviation from the dipolar case. It may be possible to optimize the pulse width for monopolar pulses, but the optimum value will in general depend on the pulse voltage.

The results of simulations close to the stability boundary are given in Fig. 9. Here the ion was placed at $q_z = 0.85$, $a_z = 0$ and the pulse width was chosen as 1.67 μs. The results show that close to the stability boundary, the optimization of the width of the dipolar pulse according to Eq. (51) is less effective in the presence of nonlinear fields, but that, unless the ion has to be brought close to the end-cap electrode, the rf phase dependence is still relatively weak. Monopolar pulses, however, show a strong rf phase dependence under these extreme conditions, and the oscillation amplitude increases nonlinearly with monopolar pulse voltage.

Holes in the end-cap electrodes, which allow injection of electrons or ions into, and ejection of ions from real ion trap devices, also cause nonlinear fields. These field faults have not been included in the simulations for Figs. 8 and 9, because their influence is limited to ions which come very close to the end-cap holes, and thus can be ignored unless the ejection of ions is investigated. The next section will address this problem.

Qualitatively the results obtained here should be comparable with experiments, in which the ion ejection efficiency was studied for varying dc pulse application times and hence different rf phases. Comparisons can be made by assuming that there is a monotonic relationship between oscillation amplitude after the dc pulse and the number of ions ejected by the pulse, viz. that the larger the oscillation amplitude in the direction of the applied pulse for a given pulse voltage, the more ions are ejected. Weil et al. used dc pulses, the width of which was short compared to the rf period [24]. They demonstrated that if a cooled ion population is subject to dc pulse excitation, the number of ions ejected from the trap varies almost sinusodially with the pulse application time and that the frequency of the variation is equal to the rf drive frequency, as expected from Eq. (46). It has also been

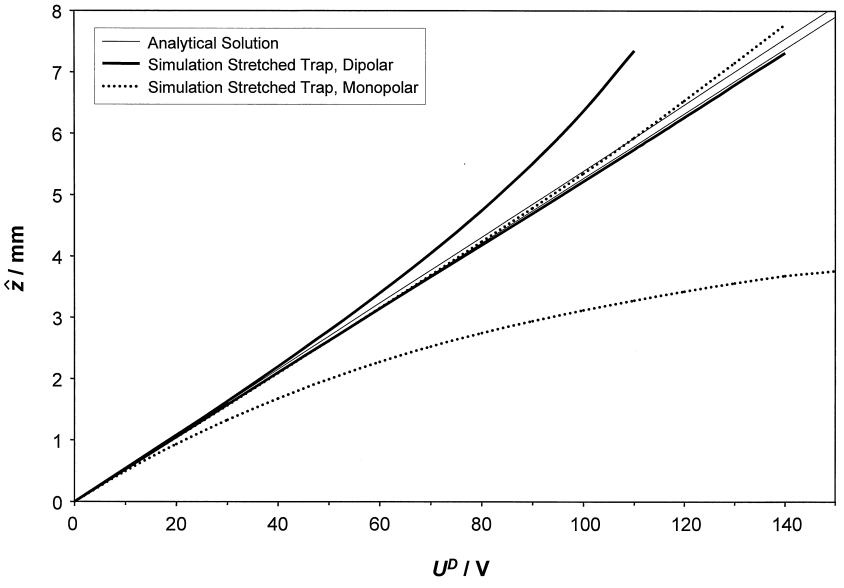

Fig. 9. Dependence of oscillation amplitude as a function of pulse voltage for an ion with a mass-to-charge ratio of 100 Th at $q_z = 0.85$, $a_z = 0$ in a stretched trap with $r_0 = 10$ mm, $z_0 = 7.83$ mm, and $\Omega/(2\pi) = 1$ MHz. The maximum and the minimum amplitude for dipolar and positive monopolar pulses with a width of 1.67 μs as obtained by simulations are shown and compared with the results of Eq. (46), which includes only a quadrupolar rf field and a dipolar dc field.

shown experimentally that, as derived above, the rf phase dependence can be greatly reduced, if the dc pulse width is chosen somewhat larger than the rf period [64]. The experimental studies by Todd and co-workers [32,59–62] are more difficult to compare with the results of the theory presented here, since they did not employ the use of a light buffer gas to cool the ion cloud to the central volume of the ion trap. Nevertheless the results of Todd et al. also show a rf phase dependence. It increases with q_z [62], which is consistent with Eq. (46), because at higher q_z the coefficients C_{2n} become larger compared to C_0. Todd et al. also noted a variation in the rf phase dependence with pulse width [60]. Qualitatively this also can be explained by Eq. (46), since, to be precise, the rf phase effect depends not on the time $t = t_0$ of the rising edge of the pulse, but on the center time $t = t_0 + \frac{1}{2}\Delta t$. However, it should be noted that they used monopolar pulses instead of dipolar pulses, and that Eq. (46) therefore does not hold strictly for their experiments. The mass [60] and pulse voltage [62] effects on the rf phase dependence observed in their studies could be due to the quadrupolar contribution of the dc pulse, as explained previously.

Overall, dc pulses are a feasible method for exciting ion motion, unless ions close to the stability boundary are of concern. There, however, the trapping efficiency is poor, so that in practice this is not a serious limitation. Dipolar pulses should be preferred over monopolar pulses. dc pulse excitation has the advantage that the duration of the excitation process is very short and thus it will not be influenced by collisions of ions with buffer gas atoms in the ion trap. However, if ions are undergoing coherent oscillations, the effect of the dc pulse depends on the secular frequency and the application time of the pulse. Therefore, care should be taken if ions are to be re-excited after a first dc pulse before the ion motion has been sufficiently dampened to the center of the trap.

7. Dc tomography

In Sec. 6, the ions have been assumed to be at the center of the ion trap prior to application of the dc pulse. Now this assumption will be removed, and it will be shown that the number of ions remaining in the

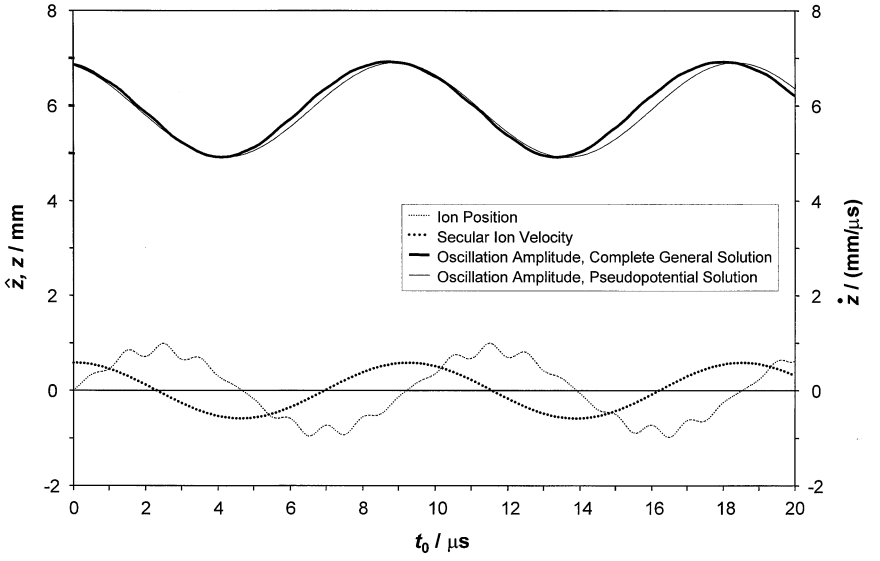

Fig. 10. Oscillation amplitude of an ion with a mass-to-charge ratio of 100 Th at $q_z = 0.3$, $a_z = 0$ under the influence of a −60 V dipolar dc pulse with a width of 1.04 μs in an ideal trap with $r_0 = 10$ mm, $z_0 = 7.07$ mm and $\Omega/(2\pi) = 1$ MHz as a function of the pulse application time t_0. The ion's position and secular velocity at t_0 are also shown.

trap after the pulse correlates with ion motion, if the pulse voltage is chosen such that a part of the ion population is ejected from the ion trap. It will be assumed that the pulse width is chosen according to Eq. (52), such that the contribution of higher order terms in the ion oscillation amplitude is small. This assumption will be validated by computer simulations.

Equation (47) describes the oscillation amplitude of an ion after application of a dipolar dc pulse in the pseudopotential approximation. Assuming that the pulse voltage is large enough for the ion to increase its oscillation amplitude significantly, i.e. if

$$\lambda_i,\ \mu_i \ll 4\,\frac{|eE^D \sin(\frac{1}{2}\bar{\omega}_{0,u}\Delta t)|}{m\bar{\omega}_{0,u}^2} \tag{53}$$

Eq. (47) can be approximated by

$$\hat{\bar{u}}_3(t_0) \approx \left|\frac{2}{(1-\frac{1}{4}q_u^2)}\frac{eE^D}{m\bar{\omega}_u^2}\sin(\tfrac{1}{2}\bar{\omega}_u\Delta t) + \frac{\dot{\bar{u}}_1^{\sec}(t_0+\Delta t)}{\bar{\omega}_u}\right| + \frac{\dot{\bar{u}}_1^{\sec}(t_0+\Delta t)}{\bar{\omega}_u}(1+\tfrac{1}{2}q_u)$$

$$= \hat{\bar{u}}_3^{\text{offset}} + \frac{\kappa}{\bar{\omega}_u}\dot{\bar{u}}_1^{\sec}(t_0+\tfrac{1}{2}\Delta t) \tag{54}$$

where

$$\hat{\bar{u}}_3^{\text{offset}} = \frac{2}{(1-\frac{1}{2}q_u)}\frac{|eE^D \sin(\frac{1}{2}\bar{\omega}_u\Delta t)|}{m\bar{\omega}_u^2} \tag{55}$$

$$\kappa = \begin{cases} +(1+\frac{1}{2}q_u) & eE^D \sin(\frac{1}{2}\bar{\omega}_u\Delta t) \geq 0 \\ -(1+\frac{1}{2}q_u) & eE^D \sin(\frac{1}{2}\bar{\omega}_u\Delta t) < 0 \end{cases} \tag{56}$$

Thus, for a fixed dc pulse voltage and pulse width, but varying times t_0 at which the pulse is applied, the resulting oscillation amplitude is given by the sum of a constant part $\hat{\bar{u}}_3^{\text{offset}}$ and a part which is proportional to the secular velocity at $t_0 + \frac{1}{2}\Delta t$. Fig. 10 illustrates this behavior for an ion with a mass-to-charge ratio of 100 Th at $q_z = 0.3$, $a_z = 0$ under the influence of a −60 V dipolar dc pulse with a width of 1.04 μs in an ideal trap with $\Omega/(2\pi) = 1$ MHz. The ion oscillation amplitude prior to the pulse is 1 mm. Note that Fig. 10 represents the result of a large number of experiments, during each of which the amplitude for a specific pulse application time t_0 is measured, and the resulting amplitudes are plotted as a function of t_0. It is evident from Fig. 10 that if the pulse width is chosen appropriately, the amplitude after dc pulse is deter-

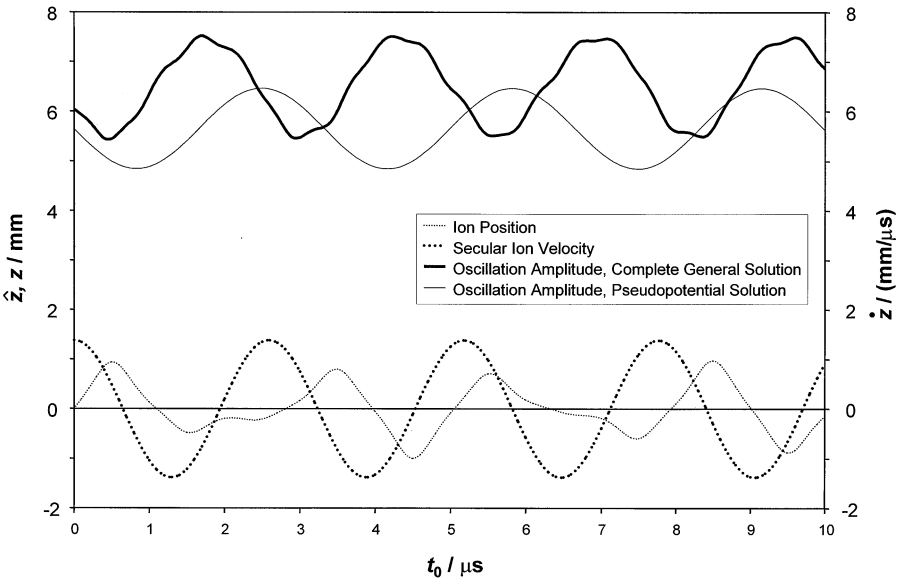

Fig. 11. Oscillation amplitude of an ion with a mass-to-charge ratio of 100 Th at $q_z = 0.85$, $a_z = 0$ under the influence of a −37.4 V dipolar dc pulse with a width of 1.67 μs in an ideal trap with $r_0 = 10$ mm, $z_0 = 7.07$ mm, and $\Omega/(2\pi) = 1$ MHz as a function of the pulse application time t_0. The ion's position and secular velocity at t_0 are also shown.

mined predominantly by the secular oscillation, rather than by the sum of secular oscillation and micromotion. Fig. 11 emphasizes this point by showing the equivalent result for $q_z = 0.85$, $a_z = 0$, a pulse voltage of −37.4 V and width of 1.67 μs. The pulse voltage has been reduced from the previous example to compensate for the larger pulse width. Although at this working point the ion motion without dipolar dc is no longer dominated by the secular oscillation but shows the strong influence of the micromotion, the amplitude still follows primarily the secular velocity. It can also be seen from Fig. 11 that the oscillation in the amplitude is shifted in phase by half the pulse width compared to the oscillation of the secular velocity.

The correlation of the oscillation amplitude after the dc pulse with the secular oscillation before the pulse can be used to probe the coherent motion of ions in the trap experimentally. If the pulse voltage is chosen such that most ions are ejected if the oscillation amplitude after the pulse is large and only few ions are ejected if the oscillation amplitude is small, the number of ejected ions and the number of ions remaining trapped after the pulse follow the secular motion. This technique, termed dc tomography, was first used by Weil et al. to probe the motion of ions in the trap and to measure their secular frequencies [23,24].

Quantitative treatment of the process requires knowledge of the phase space distribution function of the ions before and after application of the pulse. If an ion cloud is forced into coherent motion, e.g. by resonance excitation, its phase space distribution function is determined both by the width of the ion cloud prior to excitation of coherent motion and the oscillation of the center of the ion cloud. For the secular oscillation of the ion cloud center and an ion cloud with Gaussian distribution of standard deviation σ_u, the phase space distribution function can be written as

$$g(\bar{u}_1^{\mathrm{sec}}, \dot{\bar{u}}_1^{\mathrm{sec}}, t) = \frac{1}{2\pi\bar{\omega}_u\sigma_u^2} \exp\left(-\frac{[\bar{u}_1^{\mathrm{sec}} - \bar{u}_1^{\mathrm{coh}}(t)]^2}{2\sigma_u^2} - \frac{[\dot{\bar{u}}_1^{\mathrm{sec}} - \dot{\bar{u}}_1^{\mathrm{coh}}(t)]^2}{2(\bar{\omega}_u\sigma_u)^2} \right) \quad (57)$$

where position $\bar{u}_1^{\mathrm{coh}}$ and velocity $\dot{\bar{u}}_1^{\mathrm{coh}}$ of the coherent secular oscillation of the ion cloud center is given by

$$\bar{u}_1^{\mathrm{coh}}(t) = \lambda^{\mathrm{coh}} \cos(\bar{\omega}_u t) + \mu^{\mathrm{coh}} \sin(\bar{\omega}_u t) \tag{58a}$$

$$\dot{\bar{u}}_1^{\mathrm{coh}}(t) = -\bar{\omega}_u \lambda^{\mathrm{coh}} \sin(\bar{\omega}_u t) + \bar{\omega}_u \mu^{\mathrm{coh}} \cos(\bar{\omega}_u t) \tag{58b}$$

λ^{coh} and μ^{coh} determine amplitude and phase of the oscillation. It should be noted here that Eq. (57) has been chosen not to include the effects of micromotion, because the result of the dipolar dc pulse depends mainly on the velocity contribution of the secular oscillation only.

Integration of Eq. (57) over space and transformation of velocity to amplitude $\hat{\bar{u}}_3$ after application of a dipolar dc pulse at time t_0 according to Eq. (54) yields the distribution function for oscillation amplitude

$$g(\hat{\bar{u}}_3, t_0) = \frac{1}{\sqrt{2\pi}(1 + \frac{1}{2}q_u)\sigma_u} \exp\left(- \frac{\left(\hat{\bar{u}}_3 - \hat{\bar{u}}_3^{\mathrm{offset}} - \frac{\kappa}{\bar{\omega}_u} \dot{\bar{u}}_1^{\mathrm{coh}}(t_0 + \frac{1}{2}\Delta t) \right)^2}{2[(1 + \frac{1}{2}q_u)\sigma_u]^2} \right) \tag{59}$$

The number $N(t_0)$ of ions remaining in the trap after the pulse applied at $t = t_0$ is therefore given by

$$N(t_0) = \frac{N_{\max}}{\sqrt{2\pi}(1 + \frac{1}{2}q_u)\sigma_u} \int_0^{u_0} \exp\left(- \frac{\left(\hat{\bar{u}}_3 - \hat{\bar{u}}_3^{\mathrm{offset}} - \frac{\kappa}{\bar{\omega}_u} \dot{\bar{u}}_1^{\mathrm{coh}}(t_0 + \frac{1}{2}\Delta t) \right)^2}{2[(1 + \frac{1}{2}q_u)\sigma_u]^2} \right) d\hat{\bar{u}}_3 \tag{60}$$

where u_0 is the distance from the trap center to the end-cap electrode in the u direction and $N_{\max}$ the total number of ions in the trap before application of the pulse. If $\hat{\bar{u}}_3^{\mathrm{offset}} = u_0$ the variation in the ion number is symmetrical and, on average, half of the ions are ejected from the trap. According to Eq. (54), this can be achieved by choosing

$$U^D = -\frac{1 - \frac{1}{2}q_u}{2} \frac{m\bar{\omega}_u^2}{e \sin(\frac{1}{2}\bar{\omega}_u \Delta t)} \frac{r_N}{A_1^D} u_0 \tag{61}$$

Fig. 12 illustrates this case for ions with a mass-to-charge ratio of 100 Th held at $q_z = 0.3$, $a_z = 0$ in an ideal trap with $r_0 = 10$ mm, $z_0 = 7.07$ mm, and $\Omega/(2\pi) = 1$ MHz and a pulse voltage of -71.8 V for different amplitudes of the coherent oscillation. The ions were initially distributed along the z axis according to a Gaussian distribution with a standard deviation $\sigma_z = 0.4$ mm. The example shows that dc tomography can detect very small changes in the secular oscillation, in particular for oscillation amplitudes which correspond to a relative ion abundance of about 0.5. There, differences in oscillation amplitude of less than 0.1 mm should be detectable. However, the dependence of ion abundance on oscillation amplitude is nonlinear. For larger amplitudes, the differences in the changes in ion abundance get smaller, and amplitudes larger than 2 mm result in an almost rectangular signal, because either all ions are trapped or all ions are ejected. Hence, the range of positions that can be investigated is of the order of the width of the ion cloud. To monitor ion oscillations with larger amplitudes, the range of positions should be chosen close to the turning points of the coherent oscillation of the ion cloud and the pulse voltage should be adjusted accordingly. To make the dc tomography technique most sensitive for ion motion at a position u, the corresponding pulse voltage should be chosen approximately as

$$U^D = -\frac{1 - \frac{1}{2}q_u}{2} \frac{m\bar{\omega}_u^2}{e \sin(\frac{1}{2}\bar{\omega}_u \Delta t)} \frac{r_N}{A_1^D} \cdot [u_0 - (1 + \tfrac{1}{2}q_u)u] \tag{62}$$

Note that Eq. (62) was obtained for condition (53) and that adjustments to the pulse voltage are necessary if the amplitude of the coherent oscillation before the pulse is very large.

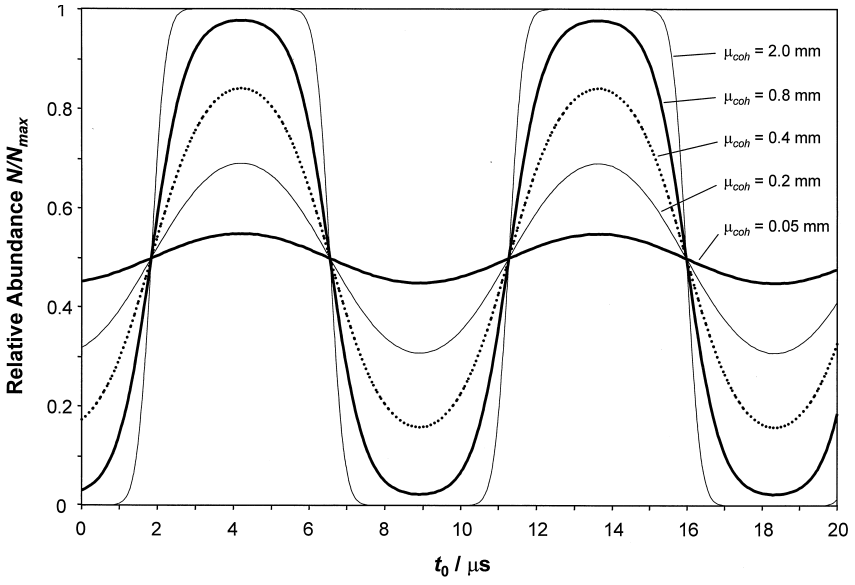

Fig. 12. Relative abundance of remaining ions after application of a dipolar pulse with a voltage of −71.8 V and width of 1.04 μs as a function of the application time t_0 of the pulse and for various amplitudes μ_{coh} of the coherent motion of the ion cloud. The phase of the coherent motion is the same as in Fig. 10. The ions with a mass-to-charge ratio of 100 Th are held at $q_z = 0.3$, $a_z = 0$ in an ideal trap with $r_0 = 10$ mm, $z_0 = 7.07$ mm, and $\Omega/(2\pi) = 1$ MHz and were initially distributed along the z axis according to a Gaussian distribution with a standard deviation $\sigma_z = 0.4$ mm.

Fig. 13 shows the relative abundance of the remaining ions for the same conditions as in Fig. 12, however a pulse voltage of −95.1 V is used to "zoom" into the region of $z = -2$ mm. Consequently, the turning points of the coherent oscillation of the ion cloud can be examined if the oscillation amplitudes are close to 2 mm. According to Eq. (60), the center of the ion cloud can be found at $z = -2$ mm at times t_0, for which the relative abundance after the pulse is 0.5.

The effect of nonlinear fields is shown in Fig. 14. Simulations for 1000 ions with a mass-to-charge ratio of 100 Th held at $q_z = 0.3$, $a_z = 0$ in a stretched trap with $r_0 = 10$ mm, $z_0 = 7.83$ mm, and $\Omega/(2\pi) = 1$ MHz were obtained as a function of the pulse application time for a pulse of 91.5 V and 1.04 μs. The analytical approximation (60) and the result of simulations, which include only the quadrupole and dipole terms with the coefficients given in Table 1 are shown. Simulations which include higher order fields were also obtained, but differ only slightly from the case of linear fields and are not shown. A larger deviation arises from the effects of holes in the end-cap electrodes. The main effect of the end-cap holes is that they lead to field penetration into the holes and thus weaken the electric field close to the end caps. The electric field increases linearly with distance from the center of the trap, but closer to the end-cap holes it levels off, decreases and goes to zero inside the end-cap holes. The transition from linear field to almost zero field is very sharp and has the overall effect that ions are ejected at a distance u_0^{eff} from the trap center, which is smaller than the closest distance u_0 from the trap center to the end caps. For the trap geometry used in the simulation with end-cap holes of 1.2 mm diameter, the ejection point is approximately $u_0^{\text{eff}} = 7.2$ mm. This value can be used in Eq. (61) to calculate the pulse voltage for the case of electrodes with end-cap holes. The results of the corresponding simulation which uses a pulse voltage of −84 V, are also given in Fig. 14. Unlike the simulations shown previously, the ions were not confined to motion on the z axis, but were also given different initial radial positions according to a standard deviation $\sigma_r = 0.4$ mm. These more realistic conditions result in no significant deviation in behavior from the idealized conditions.

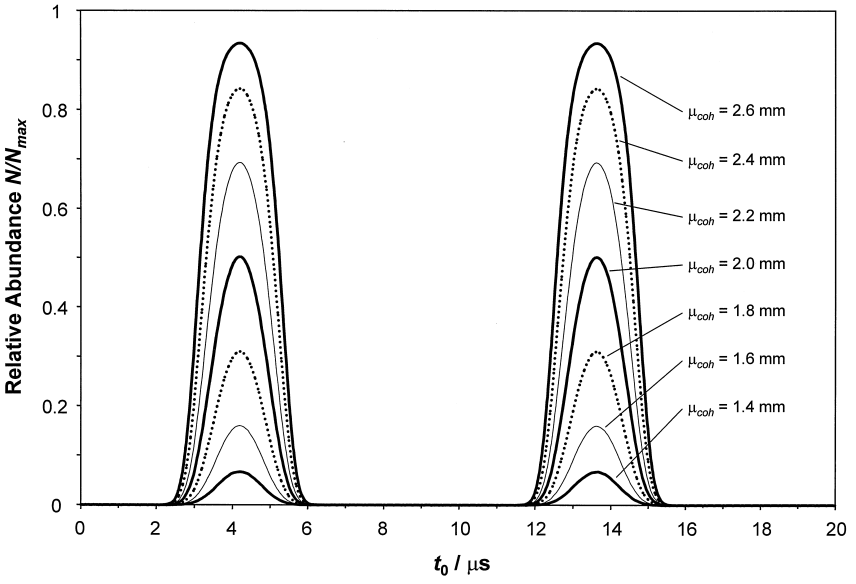

Fig. 13. Relative abundance of remaining ions after application of a dipolar pulse with an amplitude of −95.1 V and width of 1.04 μs as a function of the application time t_0 of the pulse and for various amplitudes μ_{coh} of the coherent motion of the ion cloud. The phase of the coherent motion is the same as in Fig. 10. The ions with a mass-to-charge ratio of 100 Th are held at $q_z = 0.3$, $a_z = 0$ in an ideal trap with $r_0 = 10$ mm, $z_0 = 7.07$ mm, and $\Omega/(2\pi) = 1$ MHz and were initially distributed along the z axis according to a Gaussian distribution with a standard deviation $\sigma_z = 0.4$ mm.

These results show that dc tomography is a feasible technique for probing the secular motion of ions in the ion trap. Almost sinusodial signals can be obtained, even in the presence of nonlinear fields. Weil et al. have shown that the ions' secular frequency can be measured using dc tomography [24]. They have also suggested high resolution activation and high resolution mass analysis as possible applications. Further, factors which influence the motion of ions can also be elucidated using dc tomography. For example, it is possible to measure relative collision cross sections of ions using this technique [64]. To achieve this, ions are excited into coherent oscillations in the presence of a buffer gas. In elastic collisions the ions lose kinetic energy and decrease their oscillation amplitudes. The change in amplitude can be measured by dc tomography and connected with the collision cross section.

8. Conclusions

Continuous dipolar dc fields and dipolar pulses represent a versatile method to influence the motion of ions in the rf quadrupole ion trap. They allow for a rapid increase or decrease of ion kinetic energy. It has been shown that dipolar dc pulse excitation is a broadband method over a large mass range, and that the pulse width can be chosen to avoid an rf phase dependence. Dc tomography is a technique which employs selective ejection of ions depending on the secular motion of a coherent ion cloud and thus can be used to probe the motion of ions in the ion trap. Although removal of ion kinetic energy by use of dc pulses has not been investigated in detail, the theory presented here could also be applied to problems such as the use of dc pulses to improve the trapping efficiency of ion injection.

Acknowledgements

This work was supported by the United States Department of Energy, Office of Basic Energy Sciences (contract no. DE-FG02-94ER14470). The author thanks R.G. Cooks for helpful discussions and for critically reading the manuscript.

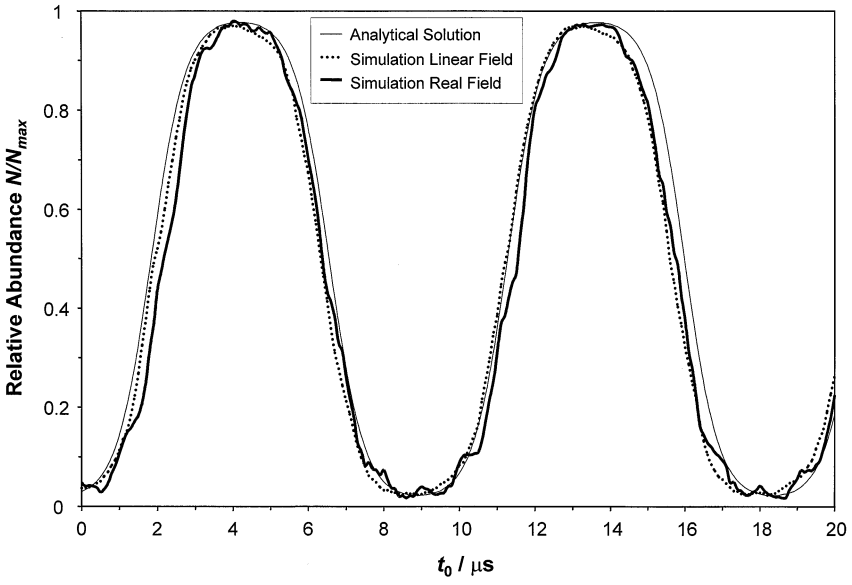

Fig. 14. Relative abundance of remaining ions after application of a 1.04 μs dipolar pulse as a function of the application time t_0 of the pulse. The amplitude of the coherent motion of the cloud is $\mu_{coh} = 0.8$ mm and the phase is the same as in Fig. 10. The ions with a mass-to-charge ratio of 100 Th are held at $q_z = 0.3$, $a_z = 0$ in a stretched trap with $r_0 = 10$ mm, $z_0 = 7.07$ mm, and $\Omega/(2\pi) = 1$ MHz and were initially distributed along the z axis according to a Gaussian distribution with a standard deviation $\sigma_z = 0.4$ mm. Shown are the analytical approximation and a simulation using 1000 ions and the quadrupole field with the superposition of the dipole field due to a −95.1 V dc pulse. Also shown is a simulation with the real field including its nonlinear contributions due to the stretched geometry and end-cap holes. To correct for the effect of the end-cap holes, the pulse voltage for this simulation was −84 V, and the ions were also spread in radial direction according to a Gaussian distribution with $\sigma_r = 0.4$ mm.

References

[1] P.H. Dawson, N.R. Whetten, J. Vac. Sci. Technol. 5 (1968) 11.
[2] G.C. Stafford, P.E. Kelley, J.E.P. Syka, W.E. Reynolds, J.F.J. Todd, Int. J. Mass Spectrom. Ion Processes 60 (1984) 85.
[3] D.B. Tucker, C.H. Hameister, S.C. Bradshaw, D.J. Hoekman, M. Weber-Grabau, Proceedings of the 36th ASMS Conference on Mass Spectrometry and Allied Topics, San Francisco, CA 1988, p. 628.
[4] J. Franzen, R.H. Gabling, M. Schubert, Y. Wang, in R.E. March, J.F.J. Todd (Eds.), Practical Aspects of Ion Trap Mass Spectrometry, Vol. 1, CRC Press, Boca Raton, FL, 1995, p. 49.
[5] J.F.J. Todd, A.D. Penman, R.D. Smith, Int. J. Mass Spectrom. Ion Processes 106 (1991) 117.
[6] U.P. Schlunegger, M. Stoeckli, R.M. Caprioli, Rapid Commun. Mass Spectrom. 13 (1999) 1792.
[7] E. Fischer, Z. Phys. 156 (1959) 1.
[8] G. Rettinghaus, Z. Angew. Phys. 22 (1967) 321.
[9] M. Soni, V. Frankevich, M. Nappi, R.E. Santini, J.W. Amy, R.G. Cooks, Anal. Chem. 68 (1996) 3314.
[10] J.E. Fulford, R.E. March, Int. J. Mass Spectrom. Ion Phys. 26 (1978) 155.
[11] R.J. Strife, P.E. Kelley, M. Weber-Grabau, Rapid Commun. Mass Spectrom. 2 (1988) 105.
[12] R.K. Julian, R.G. Cooks, Anal. Chem. 65 (1993) 1827.
[13] J.N. Louris, R.G. Cooks, J.E.P. Syka, P.E. Kelley, G.C. Stafford, J.F.J. Todd, Anal. Chem. 59 (1987) 1677.
[14] J.V. Johnson, R.A. Yost, P.E. Kelley, D.C. Bradford, Anal. Chem. 62 (1990) 2162.
[15] S.A. McLuckey, G.L. Glish, G.J. VanBerkel, Int. J. Mass Spectrom. Ion Processes 106 (1991) 213.
[16] R.E. March, F.A. Londry, R.L. Alfred, J.F.J. Todd, A.D. Penman, F. Vedel, M. Vedel, Int. J. Mass Spectrom. Ion Processes 110 (1991) 159.
[17] R.G. Cooks, C.D. Cleven, L.A. Horn, M. Nappi, C. Weil, M.H. Soni, R.K. Julian, Int. J. Mass Spectrom. Ion Processes 146/147 (1995) 147.
[18] E.R. Badman, G.E. Patterson, J.M. Wells, R.E. Santini, R.G. Cooks, J. Mass Spectrom. 34 (1999) 889.
[19] S.A. Lammert, R.G. Cooks, Rapid Commun. Mass Spectrom. 6 (1992) 528.
[20] S.A. Lammert, R.G. Cooks, J. Am. Soc. Mass Spectrom. 2 (1991) 487.
[21] S.A. Lammert, C.D. Cleven, R.G. Cooks, J. Am. Soc. Mass Spectrom. 5 (1994) 29.
[22] M. Wang, S. Schachterle, G. Wells, J. Am. Soc. Mass Spectrom. 7 (1996) 668.
[23] C. Weil, Ph.D. thesis, Justus-Liebig Universität Giessen, 1997.
[24] C. Weil, J.M. Wells, H. Wollnik, R.G. Cooks, Int. J. Mass Spectrom. 194 (2000) 225.

[25] M. Carette, P. Perrier, Y. Zerega, G. Brincourt, J.C. Payan, J. Andre, Int. J. Mass Spectrom. Ion Processes 171 (1997) 253.
[26] Y. Zerega, P. Perrier, M. Carette, G. Brincourt, T. Nguema, J. Andre, Int. J. Mass Spectrom. 190/191 (1999) 59.
[27] R.F. Bonner, G. Lawson, J.F.J. Todd, Int. J. Mass Spectrom. Ion Phys. 10 (1972) 197.
[28] S.M. Michael, B.M. Chien, D.M. Lubman, Anal. Chem. 65 (1993) 2614.
[29] Z. Ouyang, E.R. Badman, R.G. Cooks, Rapid Commun. Mass Spectrom. 13 (1999) 2444.
[30] C. Weil, C.D. Cleven, M. Nappi, H. Wollnik, R.G. Cooks, Rapid Commun. Mass Spectrom. 10 (1996) 742.
[31] R.F. Wuerker, H. Shelton, R.V. Langmuir, J. Appl. Phys. 30 (1959) 342.
[32] R.E. Mather, J.F.J. Todd, Int. J. Mass Spectrom. Ion Phys. 31 (1979) 1.
[33] S. Guan, A.G. Marshall, Int. J. Mass Spectrom. Ion Processes 157/158 (1996) 5.
[34] P.H. Dawson, N.R. Whetten, J. Vac. Sci. Technol. 5 (1968) 1.
[35] P.H. Dawson, C. Lambert, Int. J. Mass Spectrom. Ion Phys. 14 (1974) 339.
[36] H.A. Bui, R.G. Cooks, J. Mass Spectrom. 33 (1998) 297.
[37] W.R. Plass, R.G. Cooks, D.E. Goeringer, S.A. McLuckey, Proceedings of the 47th ASMS Conference on Mass Spectrometry and Allied Topics, Dallas, TX, 13–18 June 1999, p. ThPB 022.
[38] F. Vedel, J. Andre, Int. J. Mass Spectrom. Ion Processes 65 (1985) 1.
[39] Y. Moriwaki, T. Tachikawa, T. Shimizu, Jpn. J. Appl. Phys., Part 1, 35 (1996) 757.
[40] J.M. Wells, W.R. Plass, G.E. Patterson, Z. Ouyang, E.R. Badman, R.G. Cooks, Anal. Chem. 71 (1999) 3405.
[41] J.H. Billen, L.M. Young, Proceedings of the 1993 Particle Accelerator Conference, 1993, p. 790.
[42] D.J. Jackson, Classical Electrodynamics, Wiley, New York, 1975.
[43] R.D. Knight, Int. J. Mass Spectrom. Ion Phys. 51 (1983) 127.
[44] J. Louris, J. Schwartz, G. Stafford, J. Syka, D. Taylor, Proceedings of the 40th ASMS Conference on Mass Spectrometry and Allied Topics, Washington, DC, 1992, p. 1003.
[45] G. Gabrielse, Phys. Rev. A 29 (1984) 462.
[46] E.C. Beaty, Phys. Rev. A 33 (1986) 3645.
[47] Y. Wang, J. Franzen, Int. J. Mass Spectrom. Ion Processes 132 (1994) 155.
[48] M. Splendore, E. Marquette, J. Oppenheimer, C. Huston, G. Wells, Int. J. Mass Spectrom. 190/191 (1999) 129.
[49] N.W. McLachlan, Theory and Applications of Mathieu Equations, Oxford University Press, Oxford, 1947.
[50] J. Meixner, F.W. Schäfke, Mathieusche Funktionen und Sphäroidfunktionen mit Anwendungen auf Physikalische und Technische Probleme, Springer, Berlin, 1954.
[51] P.H. Dawson, in P.H. Dawson (Ed.), Quadrupole Mass Spectrometry and Its Applications, American Institute of Physics, New York, 1995, chapter 3.
[52] F.G. Major, H.G. Dehmelt, Phys. Rev. 170 (1968) 91.
[53] M. Schubert, I. Siemers, R. Blatt, Appl. Phys. B 51 (1990) 414.
[54] A.A. Makarov, Anal. Chem. 68 (1996) 4257.
[55] R.G. Cooks, A.L. Rockwood, Rapid Commun. Mass Spectrom. 5 (1991) 93.
[56] M. Nappi, V. Frankevich, M. Soni, R.G. Cooks, Int. J. Mass Spectrom. 177 (1998) 91.
[57] P.H. Hemberger, N.S. Nogar, J.D. Williams, R.G. Cooks, J.E.P. Syka, Chem. Phys. Lett. 191 (1992) 405.
[58] C.D. Cleven, R.G. Cooks, A.W. Garrett, N.S. Nogar, P.H. Hemberger, J. Phys. Chem. 100 (1996) 40.
[59] J.F.J. Todd, R.M. Waldren, Int. J. Mass Spectrom. Ion Phys. 29 (1979) 301.
[60] R.M. Waldren, J.F.J. Todd, Int. J. Mass Spectrom. Ion Phys. 29 (1979) 315.
[61] R.M. Waldren, J.F.J. Todd, Int. J. Mass Spectrom. Ion Phys. 29 (1979) 337.
[62] R.M. Waldren, J.F.J. Todd, Int. J. Mass Spectrom. Ion Phys. 31 (1979) 15.
[63] M.N. Gaboriaud, M. Desaintfuscien, F.G. Major, Int. J. Mass Spectrom. Ion Phys. 41 (1981) 109.
[64] W.R. Plass, L.A. Gill, H.A. Bui, R.G. Cooks, J. Phys. Chem. A, in press.